Proceedings of ASME 2024 Conference on Smart Materials, Adaptive Structures and Intelligent Systems
SMASIS 2024
September 9-12, 2024, Atlanta, Georgia

SMASIS2024-140338

GUIDED-WAVE STRUCTURAL HEALTH MONITORING FOR ASSESSING THE BOND STRENGTH OF INDUCTION-WELDED THERMOPLASTIC COMPOSITE JOINTS

Mattia Mazzeschi[+]
PhD Scholar & R&D Project Engineer, CIDAUT
Boecillo, Spain / Stanford University
Stanford, USA

Saman Farhangdoust*
Postdoctoral Scholar, Stanford University
Stanford, USA

Shabbir Ahmed
Postdoctoral Scholar, Stanford University
Stanford, USA

Esteban Cañibano
R&D Manager, CIDAUT
Boecillo, Spain

Maite Fernandez
Head of Dissemination and Technology Transfer, CIDAUT
Boecillo, Spain

Fu-Kuo Chang
Professor, Stanford University
Stanford, USA

ABSTRACT

This study investigates the interaction between ultrasonic guided waves (GW) propagation and bond quality of induction-welded thermoplastic composite joints. Using ultrasonic piezoelectric transducers, the proposed robust structural health monitoring (SHM) method established a strong correlation between ultrasonic signals and the health status of joint. Three joint batches were manufactured with varying shear strength by adjusting welding parameters. Batch 1 had superior properties, while batches 2 and 3 were intermediate and lower, respectively. Transducers were placed on opposite sides of the joint overlap, operating at 350 kHz and 450 kHz. Time of flight (ToF) measurements, indicating wave group velocity, showed a direct correlation with weld-line stiffness and wave propagation velocity. These findings significantly contribute to the understanding of the interaction between mechanical properties and guided wave propagation in induction-welded thermoplastic composite joints, providing valuable insights for monitoring the performance of such joints in engineering applications.

Keywords: Structural health monitoring; ultrasonic guided waves; thermoplastic composites; induction welding.

1. INTRODUCTION

Thermoplastic composites offer distinct advantages over their thermoset counterparts, including fast manufacturing processes, increased recycling capability and the opportunity for component assembly through welding[1]. Thermoplastic composite components can be joined together through a welding process that involves melting the polymeric material at their interface and consolidating the joint under pressure. This technique mitigates common challenges associated with mechanical fastening, such as stress concentrations and delaminations from hole drilling. Compared to adhesive bonding, which requires surface preparation and curing cycles, welding is more cost-effective and preserves material properties. Among the various techniques, ultrasonic [2], [3], resistance [4], [5] and induction welding [6]–[8] are considered to be most suitable for thermoplastic. Induction welding potentially allows for geometrically complex welds and does not oblige any contact with the welding stack for heating, which increases flexibility and simplifies automation [9]. Despite the advantages, composite materials are not immune to damages such as cracks and delamination caused by fluctuating or impact stresses. Contrary to metals, it is still difficult to predict the progression of damage in composite structures [9]. This poses a serious challenge in scheduling inspection intervals and planning maintenance tasks of composite aircraft structures.

Structural Health Monitoring (SHM) could enable a depth understanding of the damage progression through the integration of sensors in the monitored structure and acquiring and analyzing the produced data during the service life to inform about damage existence, localization and type.

Ultrasonic guided waves (GW) are recognized for their significant potential in detailed quantitative structural health monitoring (SHM)[10]. Current research focuses on establishing a reliable correlation between variations in GW propagation and real-world defects in joints [11], [12]. Several significant studies[13]–[15] have investigated the interaction of ultrasonic GW with adhesively bonded single-lap metallic joints. These studies have demonstrated that both group velocity and

Corresponding authors:
[+] matmaz@cidaut.es
*sfarhang@stanford.edu

characteristic frequency shift can serve as effective measures for quantifying adhesive bond strength, particularly in joints produced with varying surface treatments [13], [14]. Additionally, these parameters have shown promise in detecting defects such as kissing bonds [15].

There is limited research on the application of ultrasonic GW for evaluating the integrity of welded thermoplastic joints: P. Ochôa et al. [16] conducted a study on GW propagation in ultrasonically welded thermoplastic composite joints. The key finding of this research is the ability to detect and differentiate between two defective scenarios by analyzing Time of Flight (ToF). The higher ToF in joints with unwelded areas indicates a slower wave group velocity and correlates with lower failure loads in single-lap tests, highlighting ToF's sensitivity to changes in joint stiffness.

To date, no studies have been found regarding the application of GW for evaluating induction-welded joints. The aim of this study is to explore the interaction between ultrasonic GW propagation and bondline characteristics of thermoplastic induction welded joints across varying levels of weld strength. Specifically, the focus is on examining the correlation between time of flight (ToF) measurements and weld strength.

2. MATERIALS AND METHODS

2.1 Materials and processing

The composite material employed to fabricate the welded samples comprised 2.5 mm thick Carbon Fiber Reinforced Thermoplastic (CFRTP) laminates with a polyphenylene sulphide polymer (PPS) matrix and a five-ply satin-woven carbon fibre, sourced from Toray Industries, Inc. The dimensions of the samples for welding were 240 mm by 100 mm. Samples were welded in a single overlap configuration with a nominal overlap of 13 mm. Welding was performed using a commercial induction welding machine, which incorporates an integrated multifunctional controller driving a solid-state frequency generator. Energy transfer to the CFRP laminates was achieved via a solenoid inductor, manipulated by an industrial robot (KUKA). Adequate air cooling was employed to prevent overheating of the upper surface of the workpiece (Fig.1), and a pressure application system comprising two rollers completed the consolidation process.

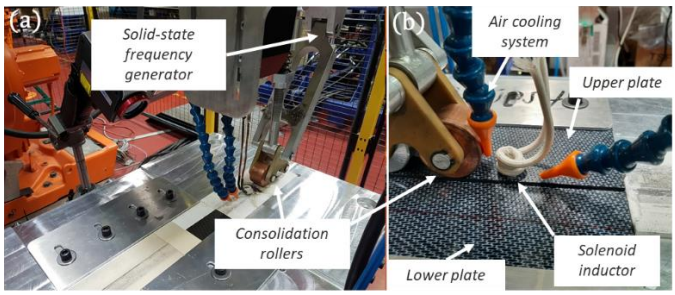

FIGURE 1: (a) PANORAMIC AND (b) DETAIL VIEW OF THE INDUCTION WELDING SYSTEM.

Three different sets of parameters were utilized to create three batches with varying mechanical properties, as detailed in Table 1. The solenoid inductor was supplied with an alternating frequency of 186 kHz. Batch 1 welding parameters were established based on prior studies [17], [18] with the aim to manufacture joints serving as a reference state for this investigation. The inductor power and rollers pressure were then adjusted to control the quality of the following batches.

TABLE 1 WELDING PROCESS CONTROL PARAMETERS FOR THE THREE BATCHES.

	Coupons per batch	Inductor power [kW]	Rollers pressure [MPa]	Inductor frequency [kHz]
Batch 1	3	1.9	2.5	186
Batch 2	3	1.2	2.5	186
Batch 3	3	1.9	1.7	186

Power input plays a crucial role in the process as it directly influences the heat generation in a specific material region, with heat being proportional to the generated power in that area. The power is directly correlate with the heating time, influencing polymer movement at the weld interface. When maintaining constant inductor speed, a higher power heat input leads to a longer residence time, improving weld quality by facilitating increased polymer chain migration [6], [19]. However, excessive power input must be avoided to prevent resin degradation, necessitating a balanced approach. Conversely, insufficient power input lead to poor wetting and low strength. Taking into account these factors, the inductor power was lowered when transitioning from Batch 1 to Batch 2, aiming to produce a joint with a deliberately reduced lap-shear strength.

Relative to roller pressure application, appropriate pressure ensures quality consolidation, facilitating intimate contact between the CFRTP adherents. However, excessive pressure can compromise weld quality, leading to increased matrix squeeze-out. Inadequate pressure application can lead to inadequate consolidation of the matrix, resulting in voids in the bondline [8], [20]. To intentionally produce a batch with minimal lap shear strength reduction, roller pressure was reduced from batch 1 to batch 3.

After welding, the welded adherents underwent machining to achieve lap joints with a nominal width of 25.4 mm, intended for initial ultrasonic guided waves testing followed by lap-shear testing. The welded joints were mechanically tested according to the ASTM D1002 standard in a MTS QTEST 159 universal testing machine, in order to obtain the single lap shear strength (LSS). Photographs of the fracture surfaces were taken using a Alicona Infinite Focus SL optical 3D measurement system and Zeiss Stemi 2000-C microscope.

2.2 Ultrasonic guided waves testing

The full ultrasonic guided waves (GW) testing setup is shown in Fig. 2. Acellent's ScanGenie Mini (SG Mini) hardware was employed for ultrasonic excitation of a piezo-ceramic (PZT) transducer. The same type of PZT transducer was used to sense

the ultrasonic response, which was also acquired by SG Mini. The collected data were then processed using Acellent's software.

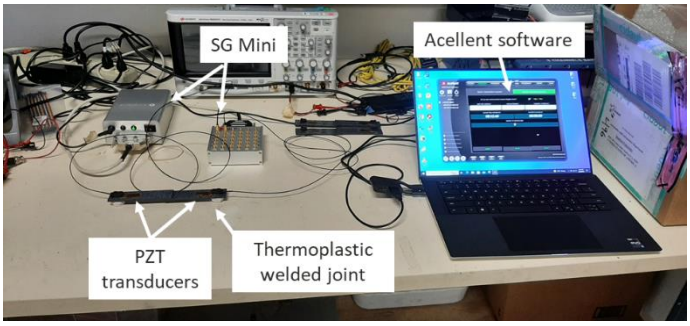

FIGURE 2: FULL SET-UP USED FOR ULTRASONIC GUIDED WAVE TESTING.

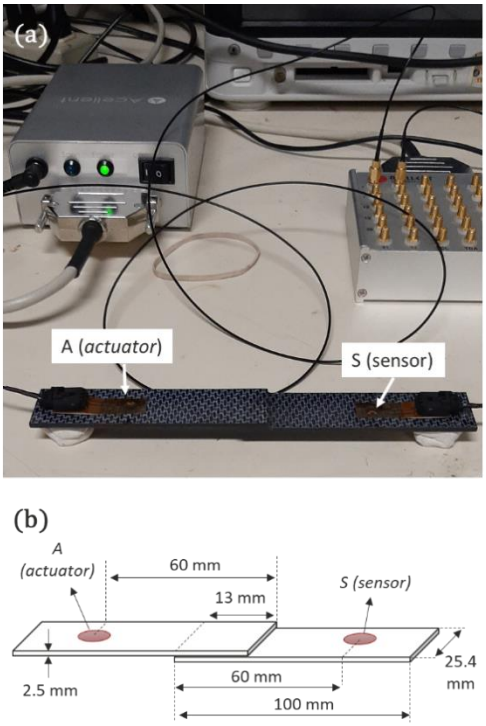

FIGURE 3: (a) SINGLE-LAP JOINT INSTRUMENTED WITH PZT TRANSDUCERS, ONE FUNCTIONING AS ACTUATOR AND THE OTHER AS SENSOR. (b) SCHEMATIC VIEW WITH DIMENSIONS.

The PZT transducers were bonded to the CFRTP adherends at the positions indicated in Fig. 3. Specifically, Fig. 3 (b) illustrates a schematic representation of the PZT transducer placement alongside the dimensions of the welded joint coupons. Each batch included three specimens, each equipped with a pair of PZT transducers. Ultrasonic GW testing was conducted prior to conducting destructive mechanical tests on the specimens. The excitation signal comprised a sinusoidal tone-burst with a 10-cycle Hanning window amplitude modulation generated at two frequencies: 350 kHz and 450 kHz. Based on the dispersion curves from [21] which were derived for comparable CF/PPS welded plates, lamb waves are expected in symmetrical and asymmetrical modes exhibiting GW modes up to order one in the adherent and modes up to order two in the overlap region. The excitation frequencies of 350 kHz and 450 kHz were meticulously chosen based on an analysis of the ToF parameter variation as detailed in [21]. Specifically, we focused on frequencies that demonstrated significant variation in ToF across different batches of CF/PPS welded specimens described in [21], while considering their identical nature except for thickness differences. Our aim was to select frequencies that yielded product excitation frequency multiplied by thickness values in a range similar to the optimal values observed in [21]. This selection process ensured alignment with frequencies showing superior sensitivity and minimal result dispersion in previous research, thereby enhancing the effectiveness of detecting variations in joint quality. Testing at two distinct frequencies, helped in investigating the interaction between various GW modes and the quality of the welded line. This approach aimed to identify the frequency that offers superior sensitivity and minimal result dispersion.

3. RESULTS AND DISCUSSION

3.1 Welded lap-joints assessment

Fig. 4 displays the results of the single-lap shear tests. The maximum load carried by the specimens during the single-lap shear tests was divided by the total overlap area to derive the apparent LSS. As expected, batch 1 serves as the reference state, exhibiting higher average LSS values at approximately 27.3 MPa. In contrast, batch 2, utilizing a lower power input, shows reduced average LSS values around 23.5 MPa. This reduction may be attributed to the shorter exposure time of the workpiece to the induction field, leading to reduced molecular inter-diffusion of polymer chains between the welding partners. Batch 3 lap joints exhibit the lowest average LSS values around 13.6 MPa due to insufficient consolidation resulting from the lowest application pressure.

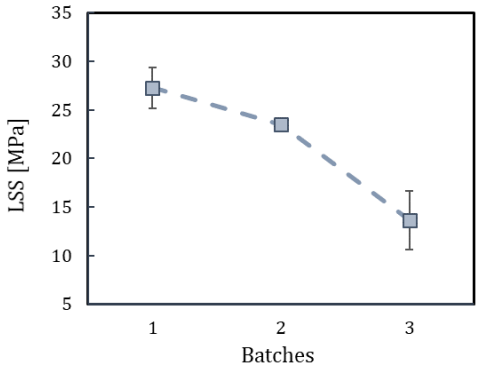

FIGURE 4: LAP SHEAR STRENGTH FOR EACH BATCH.

Considerations must be given to the fact that in this welding technique, electromagnetic waves traverse the adherents to reach the welding interface. Inductive phenomena are sensitive to substrate characteristics like material type, thickness, and

quality, potentially explaining the high scatter in lap shear test results. Additionally, non-uniformities in welded joints due to the transient nature of welding processes may interact with uneven stress distribution in the joints, influencing test results. Specifically, among the three batches, batch 1 and 3 exhibit greater scatter than batch 2. The higher power inputs in batches 1 and 2 may lead to more variability in the welding process, affecting temperature distribution, resin flow, and consolidation, resulting in a wider range of bonding qualities. Conversely, lower power input in batch 2 leads to a more consistent and controlled welding process, resulting in reduced dispersion in LSS values.

Careful evaluation of LSS results is essential, particularly considering that the stress distribution is not uniform at the bondline. Peel and shear stress concentrations at the overlap edges in single-lap shear tests are highly sensitive to factors like joint geometry (taper, fillet, and bondline thickness) and the stiffness of the bondline and adherend [22], influencing the failure mechanism. Therefore, analyzing fracture surfaces is a valuable tool to understand the mechanical performance of welds and aids in interpreting ultrasonic GW results. Fig. 5 and Fig. 6 show fracture surface analysis respectively for batch 1 and 2, revealing intralaminar failure and mesh tearing. The observed fracture features indicate successful bondline consolidation, notably evident in batch 1 where significant intralaminar failure is observed. In fact, the higher pressure applied in comparison to batch 3 indicates improved weld consolidation. Conversely, batch 3's fracture surface (Fig. 7) reveals voids and air pockets due to insufficient consolidation, along with a lack of intralaminar failures indicating poor resin flow from the substrates.

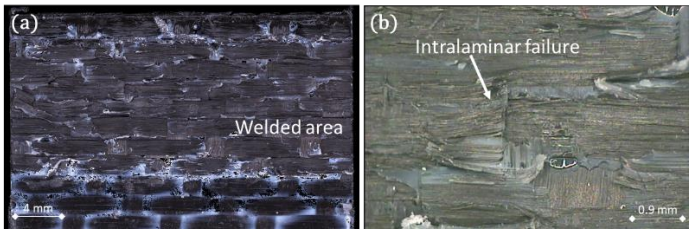

FIGURE 5: FRACTURE SURFACE ANALYSIS OF THE WELDED AREA FOR BATCH 1, INCLUDING BOTH (a) GENERAL OVERVIEW AND (b) DETAILED VIEW.

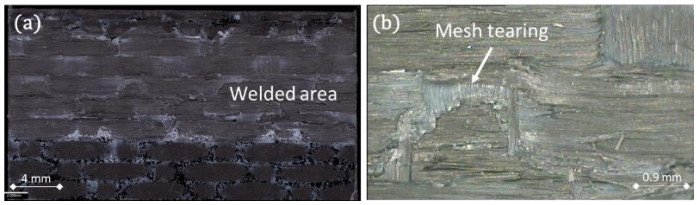

FIGURE 6: FRACTURE SURFACE ANALYSIS OF THE WELDED AREA FOR BATCH 2, INCLUDING BOTH (a) GENERAL OVERVIEW AND (b) DETAILED VIEW.

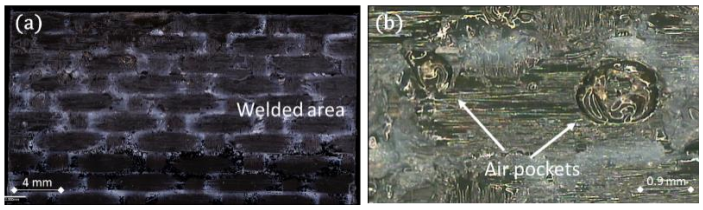

FIGURE 7: FRACTURE SURFACE ANALYSIS OF THE WELDED AREA FOR BATCH 3, INCLUDING BOTH (a) GENERAL OVERVIEW AND (b) DETAILED VIEW.

3.2 Ultrasonic guided wave detection

In order to study the interaction between UGW propagation and the welded line, GW signals were analyzed in the time domain by exploring how the ToF parameter varies for different level of the lap-joint strength.

Due to the anisotropy of composite material, particle motion along one direction can induce motion in a perpendicular direction due to the varying fiber orientation across the laminate's thickness [9]. This coupling results in all GW modes being interconnected. Therefore, discerning the distinct GW modes and establishing their correlation with welded line quality becomes intricate.

Following the approach reported in [21], the ToF was defined as the temporal duration between the peak amplitude point of the excitation pulse ($t_{max,sens}$) and the corresponding peak amplitude point of the sensed signal ($t_{max,exc}$) (see Fig. 8 and Fig. 9):

$$ToF = t_{max,sens} - t_{max,exc} \quad (1)$$

This approach establishes a direct correlation between ToF and group velocity, avoiding the need for specific GW mode group velocity calculations. The peak amplitude point in the sensed signal can correspond to a directly arriving GW mode's peak amplitude or result from constructive interference involving direct arrival, reverberation, or reflection, or both. Nonetheless, discrepancies in the time of occurrence of this peak amplitude point at a given frequency indicate changes in one or more GW mode's group velocity. Thus, this method of defining TOF differences enables indirect assessment of group velocity changes. Consequently, it was decided to use the raw data without additional signal processing to maintain the integrity of the information captured during testing.

The results of ToF are reported in Fig. 10 for all considered batches at both excitation frequencies. Across both frequencies examined, there is a discernible upward trend from batch 1 to batch 3. This trend is exactly the opposite of what was already observed in LSS values (Fig. 4), where batch 1 specimens consistently exhibit significantly higher failure loads compared to those in batches 2 and 3. Considering the inverse relationship between ToF and group velocity, a decrease of group velocity is found to be correlated with a decrease in bond strength.

However, the high standard deviation of the mean values at 350 kHz makes difficult to establish an unequivocal trend.

The only discernible change in ToF, enabling the establishment of an unambiguous increment, occurs when transitioning from the reference state (batch 1) to the batch with the lowest LSS values (batch 3). With an increase in excitation frequency to 450 kHz, the scattering of results diminishes, facilitating a clearer identification of the ToF increase from batch 1 to batch 2 by approximately 11 μs and from batch 1 to batch 3 by about 13 μs. Despite this, batch 3 specimens still exhibit greater variability, making it challenging to distinguish them from batch 2 specimens.

The high scattering of ToF values characterizing batch 3 at both frecuencies could be attribuited to the irregularities and interruptions caused by the presence of porosity as highlighted in Fig. 7. Porosity or air pockets act as interfaces with different acoustic impedance, leading to partial reflection and refraction of UGW. This alters wave propagation paths and introduces scattering effects, contributing to a broader distribution of wavefronts and a more complex wave pattern. Additionally, air-filled regions cause increased attenuation of ultrasonic waves due to the lower acoustic impedance of air compared to solid materials. This attenuation reduces signal amplitudes, alters waveforms, and can distort phase characteristics, posing challenges in accurate ToF measurements and signal interpretation. Moreover, scattering the waves sideways could induce extra reflections from the overlap edges. The presence of additional reflections is evident from the greater number of narrow wave packets observed in the signals of batch 3, contrasting with signals from batches 1 and 2, as depicted in Fig. 8 (c) and Fig. 9 (c).

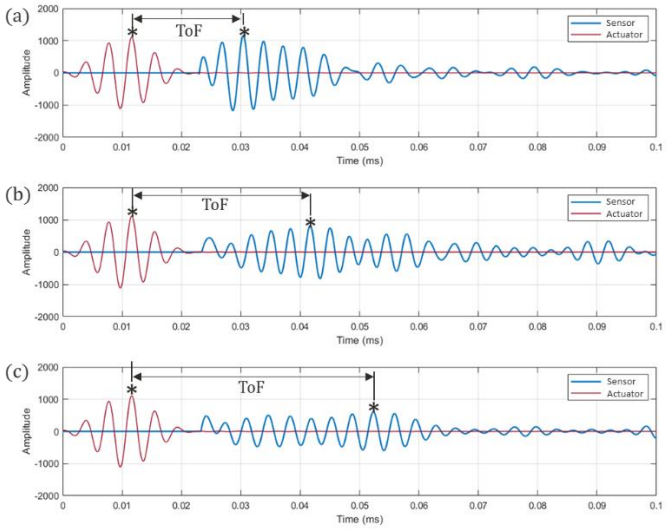

FIGURE 8: ULTRASONIC GW SIGNALS OF SENSOR (BLUE LINE) AND ACTUACTOR (RED LINE) AT 350 KHZ FROM (a) BATCH 1, (b) BATCH 2 AND (c) BATCH 3.

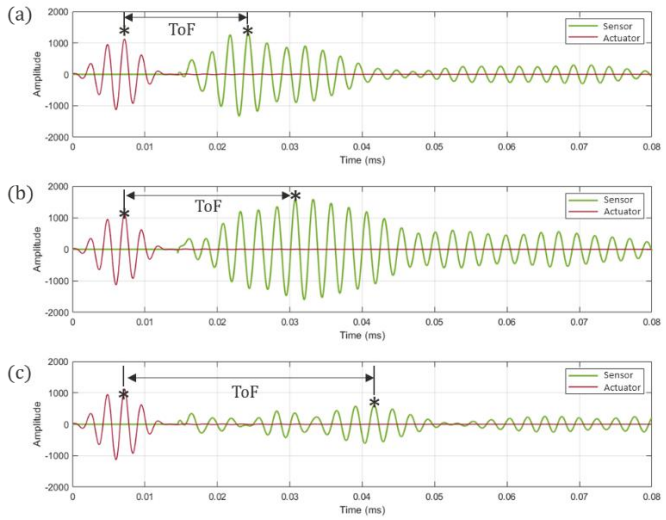

FIGURE 9: ULTRASONIC GW SIGNALS OF SENSOR (GREEN LINE) AND ACTUACTOR (RED LINE) AT 450 KHZ FROM (a) BATCH 1, (b) BATCH 2 AND (c) BATCH 3.

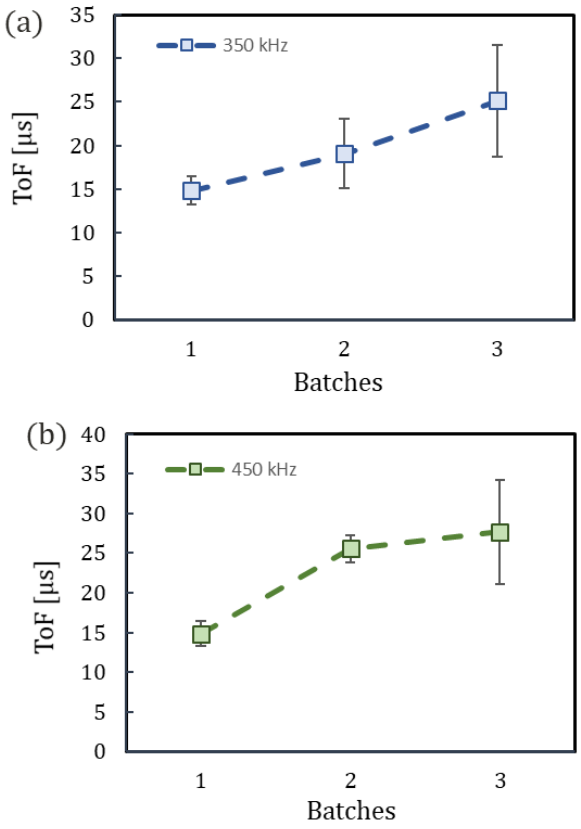

FIGURE 10: TIME-OF-FLIGHT FOR THE THREE BATCHES AT (A) 350 KHZ AND (B) 450 KHZ EXCITATION FREQUENCY.

The Fig. 11 illustrates the relationship between ToF values and LSS values, with linear interpolation lines for both frequencies. Although there is some scattering, particularly noticeable at low LSS values, a clear decreasing trend in ToF is

discernible for both frequencies as the strength of the joint increases. This finding indicates a consistent decrease in group velocity with diminishing bond strength, highlighting the correlation between ToF and joint integrity. The interpolation curve derived from the dataset analyzed in this study presents a promising avenue for quantifying LSS based on ToF values in ultrasonic guided wave testing. This curve could serve as a potential approach for estimating LSS non-destructively. However, it's crucial to note that obtaining calibration curves with a high confidence level requires thorough testing with a larger number of specimens. Further experimentation and validation using diverse specimen sets would enhance the robustness and reliability of the relationship between ToF and joint integrity.

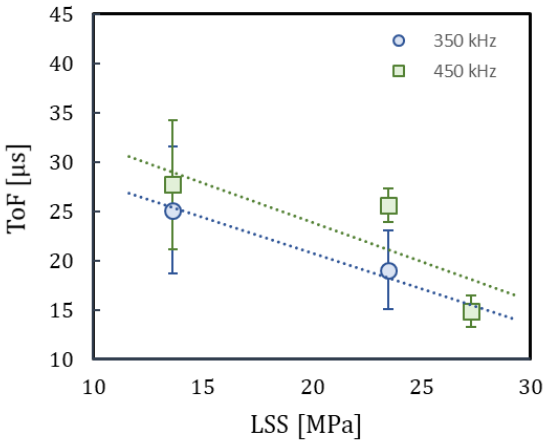

FIGURE 11: TOF VS LSS FOR THE ALL CONSIDERED BATCHES AND EXCITATION FREQUENCIES.

4. CONCLUSION

In this paper, the correlation between an appropriately defined ToF GW parameter and the weld strength of thermoplastic induction welded joints is investigated Various batches of specimens were manufactured to vary the weld strength, and the GW signals passing through the joint overlap were evaluated. A consistent relationship between ToF and Lap Shear Strength (LSS) was observed. These findings suggest an increased potential for utilizing ultrasonic guided wave-based SHM techniques to evaluate the bond strength of induction-welded thermoplastic composite joints. Furthermore, there is significant potential to utilize these techniques for real-time monitoring of the welding process itself. This includes assessing variations in ultrasonic GW characteristics between structurally sound joints and those with defects.

ACKNOWLEDGEMENTS

The authors would like to extend their sincere appreciation to Dr. Pu Xie for his support in the activities related to test setup installation. Authors would like to acknowledge the mentoring support under Visiting Student Researchers (VSR) program provided by Aeronautics and Astronautics Department at Stanford University.

REFERENCES

[1] M. Favaloro, “A comparison of the environmental attributes of thermoplastic vs. thermoset composites,” *Int. SAMPE Tech. Conf.*, pp. 1–6, 2009.

[2] S. K. Bhudolia, G. Gohel, K. F. Leong, and A. Islam, “Advances in ultrasonicwelding of thermoplastic composites: A review,” *Materials (Basel).*, vol. 13, no. 6, 2020, doi: 10.3390/ma13061284.

[3] Y. Wang, Z. Rao, S. Liao, and F. Wang, “Ultrasonic welding of fiber reinforced thermoplastic composites: Current understanding and challenges,” *Composites Part A: Applied Science and Manufacturing*, vol. 149. Elsevier Ltd, 2021. doi: 10.1016/j.compositesa.2021.106578.

[4] D. Brassard, M. Dubé, and J. R. Tavares, “Resistance welding of thermoplastic composites with a nanocomposite heating element,” *Compos. Part B Eng.*, vol. 165, pp. 779–784, 2019, doi: 10.1016/j.compositesb.2019.02.038.

[5] X. Xiong *et al.*, “Resistance welding technology of fiber reinforced polymer composites: a review,” *Journal of Adhesion Science and Technology*, vol. 35, no. 15. Taylor and Francis Ltd., pp. 1593–1619, 2021. doi: 10.1080/01694243.2020.1856514.

[6] T. J. Ahmed, D. Stavrov, H. E. N. Bersee, and A. Beukers, “Induction welding of thermoplastic composites-an overview,” *Compos. Part A Appl. Sci. Manuf.*, vol. 37, no. 10, pp. 1638–1651, 2006, doi: 10.1016/j.compositesa.2005.10.009.

[7] T. Bayerl, M. Duhovic, P. Mitschang, and D. Bhattacharyya, “The heating of polymer composites by electromagnetic induction - A review,” *Composites Part A: Applied Science and Manufacturing*, vol. 57. pp. 27–40, 2014. doi: 10.1016/j.compositesa.2013.10.024.

[8] S. Becker, M. Michel, P. Mitschang, and M. Duhovic, “Influence of polymer matrix on the induction heating behavior of CFRPC laminates,” *Compos. Part B Eng.*, vol. 231, 2022, doi: 10.1016/j.compositesb.2021.109561.

[9] L. Moser, P. Mitschang, and A. Schlarb, “Robot based induction welding of thermoplastic polymer composites,” *Int. SAMPE Symp. Exhib.*, vol. 52, Jan. 2008.

[10] Farhangdoust, S., Tashakori, S., Baghalian, A., Mehrabi, A., & Tansel, I. N. (2019, March). Prediction of damage location in composite plates using artificial neural network modeling. In Sensors and Smart Structures Technologies for Civil, Mechanical, and Aerospace Systems 2019 (Vol. 10970, pp. 100-110). SPIE.

[11] Z. Su, L. Ye, and Y. Lu, “Guided Lamb waves for identification of damage in composite structures: A review,” *J. Sound Vib.*, vol. 295, pp. 753–780, Aug.

2006, doi: 10.1016/j.jsv.2006.01.020.
[12] M. Mitra and S. Gopalakrishnan, “Guided wave based structural health monitoring: A review,” *Smart Mater. Struct.*, vol. 25, no. 5, 2016, doi: 10.1088/0964-1726/25/5/053001.
[13] L. Singher, Y. Segal, E. Segal, and J. Shamir, “Considerations in bond strength evaluation by ultrasonic guided waves,” *J. Acoust. Soc. Am.*, vol. 96, no. 4, pp. 2497–2505, 1994, doi: 10.1121/1.410123.
[14] L. Singher, “Bond strength measurement by ultrasonic guided waves,” *Ultrasonics*, vol. 35, no. 4, pp. 305–315, 1997, doi: 10.1016/S0041-624X(96)00109-6.
[15] T. Kundu, “Ultrasonic and electromagnetic waves for nondestructive evaluation and structural health monitoring,” *Procedia Eng.*, vol. 86, pp. 395–405, 2014, doi: 10.1016/j.proeng.2014.11.053.
[16] P. Ochôa, I. F. Villegas, R. M. Groves, and R. Benedictus, “Diagnostic of manufacturing defects in ultrasonically welded thermoplastic composite joints using ultrasonic guided waves,” *NDT E Int.*, vol. 107, 2019, doi: 10.1016/j.ndteint.2019.102126.
[17] M. Mazzeschi, K. C. Nuñez, E. Cañibano, and J. C. Merino, “Monitoring of thermoplastic induction welding defects. Use of electromagnetic properties as a predictive tool,” *Struct. Heal. Monit.*, vol. 0, no. 2, pp. 1–15, 2022, doi: 10.1177/14759217221111979.
[18] M. Mazzeschi, K. Nuñez-Carrero, M. Peña, E. Cañibano, and J. C. Senovilla, “Thermoplastic weld fatigue behaviour analysis using structural health monitoring sensors data,” in *Proceedings of MATCOMP21 (2022) and MATCOMP23 (2023)*, 2024, p. Vol. 08.
[19] T. Zach, J. Lew, T. H. North, and R. T. Woodhams, “Joining of high strength oriented polypropylene using electromagnetic induction bonding and ultrasonic welding,” *Mater. Sci. Technol.*, vol. 5, no. 3, pp. 281–287, Mar. 1989, doi: 10.1179/mst.1989.5.3.281.
[20] C. Ageorges, L. Ye, and M. Hou, “Advances in fusion bonding techniques for joining thermoplastic matrix composites: A review,” *Compos. - Part A Appl. Sci. Manuf.*, vol. 32, no. 6, pp. 839–857, 2001, doi: 10.1016/S1359-835X(00)00166-4.
[21] P. Ochôa, I. F. Villegas, R. M. Groves, and R. Benedictus, “Diagnostic of manufacturing defects in ultrasonically welded thermoplastic composite joints using ultrasonic guided waves,” *NDT E Int.*, vol. 107, 2019, doi: 10.1016/j.ndteint.2019.102126.
[22] L. F. M. Silva, M. Costa, G. Viana, and R. Campilho, “Chapter 2 . Analytical Modelling for the Single-Lap Joint,” 2016. doi: 10.1201/9781315370835-3.